Slow light in dielectric composite materials of metal nanoparticles

Kwang-Hyon Kim,[1,2] Anton Husakou,[1] and Joachim Herrmann[1,*]

[1]*Max Born Institute for Nonlinear Optics and Short Pulse Spectroscopy, Max-Born-Str. 2a, Berlin D-12489, Germany*
[2]*Coherent Optics Department, Institute of Lasers, State Academy of Sciences, Unjong District, Pyongyang, DPR Korea*

(Dated: September 18, 2012)

We propose a method for slowing down light pulses by using composites doped with metal nanoparticles. The underlying mechanism is related to the saturable absorption near the plasmon resonance in a pump-probe regime, leading to strong dispersion of the probe refractive index and significantly reduced group velocities. By using the non-collinear scheme, it is possible to realize the total fractional delay of 43 or larger values. This scheme promises simple and compact slow-light on-chip devices with tunable delay and THz bandwidth.

PACS numbers 78.67.Sc, 42.25.Bs, 73.20.Mf, 78.40.Pg

Recently, slow light [1, 2] has attracted much attention because of its fundamental significance and promising long-reaching applications including all-optical storage, switching and data regeneration in telecommunications, enhancement of interferometers performance and of nonlinear optical processes. It has been observed using different physical mechanisms such as electromagnetically induced transparency [3, 4], coherent population oscillations (CPO) [5–7], stimulated Brillouin [8] and Raman scattering [9], photonic crystal waveguides [10, 11], fiber Bragg gratings [12], double resonances [13] and others. The existing methods, however, are restricted to diverse limitations, most notably large propagation length (such as km-scale fibers for Brillouin scattering), small operation bandwidth (for example, $2 \sim 50$ MHz in electromagnetically induced transparency), as well as long pulse durations and others that must be circumvented for a given application. In particular, for practical applications, miniaturized designs of the delay line and its integration in optical networks are requested, that can be mass-produced and will work reliably under varying conditions. Recently progress into this direction has been achieved by the realization of on-chip delay based on different schemes [4, 14, 15].

In the present paper we propose a new approach for the realization of a slow-light device which relies on composite materials doped with metal nanoparticles (NPs). In such composites the absorption near the plasmon resonance becomes saturated with increasing intensity [16, 17], because the light-induced nonlinear change of the metal dielectric function leads to a shift of the plasmon resonance [17]. The key feature of the considered system is the retarded nonlinear response of metals in the ps time range. Therefore in the pump-probe regime the permittivity will show large-amplitude oscillations, if pump and probe frequencies are sufficiently close. As a consequence, a THz-scale dip induces in a homogeneously broadened spectral shape, and (due to Kramers-Kronig relations) a steep change of the effective refraction index near the probe wavelength, leading to a significant slowing down.

We consider a dielectric composite doped with small metal NPs, which is illuminated by two waves: the strong quasi-continuous-wave pump E_0 and the weak pulsed probe $E_{\rm pr}(t)$ with a central frequency slightly off-set from that of the pump. The main feature in the optical response of these materials is the excitation of plasmons in the spectral range of the plasmon resonance which is responsible for the enhancement of the local electromagnetic field in the vicinity of the NPs [18]. The total enhanced field in the NPs can be written as $E^{\rm enh}(t) = E_0^{\rm enh} e^{-i\omega_0 t} + E_{\rm pr}^{\rm enh}(t)\, e^{-i\omega_{pr} t}$. Here we assume $\left|E_0^{\rm enh}\right|^2 \gg \left|E_{\rm pr}^{\rm enh}\right|^2$ with a beat frequency $\Omega = \omega_0 - \omega_{pr}$ much smaller than ω_0 and ω_{pr}. The transient nonlinear change of dielectric function of metal can be described as

$$\Delta\varepsilon_m(t) = \frac{\chi_m^{(3)}}{\tau}\int_{-\infty}^{t} \left|E^{\rm enh}(t')\right|^2 e^{-\frac{t-t'}{\tau}} dt', \quad (1)$$

where τ is the electron-phonon coupling time in the range of 1-3 ps [19] and $\chi_m^{(3)} = \chi_m^{(3)}(\omega_0;\omega_0,-\omega_0,\omega_0)$ is the inherent third-order nonlinear susceptibility of the metal NPs at the pump wavelength. In this paper we consider picosecond pulses and therefore the electron-electron scattering process with a response time of few fs can be neglected. The corresponding transient dielectric function of the metal is therefore described by

$$\varepsilon_m(t) = \varepsilon_{m0} + \chi_m^{(3)}\left\{\left|E_0^{\rm enh}\right|^2 + 2{\rm Re}\left[E_0^{\rm enh*}\tau^{-1}e^{i\Omega t}\times \int_{-\infty}^{0} E_{\rm pr}^{\rm enh}(t+t')\, e^{\left(i\Omega+\frac{1}{\tau}\right)t'} dt'\right]\right\}, \quad (2)$$

where ε_{m0} is the linear dielectric function of metal. From the above equation, one can see that $\varepsilon_m(t)$ (and therefore the effective index) oscillates as $\cos\Omega t$. As a result, a part of the pump beam energy is transferred to the probe through two-beam coupling. Correspondingly, the total transmittance of the probe is increased. This principle shows a certain analogy with coherent population oscillations (CPO) in two level systems, but the essential difference here is that the two beam coupling arise by the nonlinear excitation of surface plasmons and the saturable absorption do not arise by population inversion but by the nonlinear shift of the plasmon resonance. The absorption

dip in this mechanism is created in nanocomposites with a *homogeneous* plasmonic absorption profile by *coherent coupling* between pump and probe, being substantially different from the slow light mechanism based on spectral hole burning [20], in which an absorption dip originates from the selective bleaching of a homogeneous line in the inhomogeneously broadened absorption spectrum without any coherent beam coupling.

Separating the spectral components at ω_0 and ω_{pr} in the electric displacement $D_m(t) = \varepsilon_m(t) E^{\rm enh}(t)$, we find

$$\begin{aligned} \varepsilon_m(\omega_0) &= \varepsilon_{m0} + \chi_m^{(3)} \left|E_0^{\rm enh}\right|^2, \\ \varepsilon_m(\omega_{pr}) &= \varepsilon_{m0} + \chi_m^{(3)} \left(1 + \tfrac{1}{1+i\Omega\tau}\right) \left|E_0^{\rm enh}\right|^2. \end{aligned} \quad (3)$$

For spherical metallic NPs with diameters smaller than 10 nm, the field enhancement factor (the ratio of enhanced field to the incident field) is given by $x = 3\varepsilon_h/(\varepsilon_m + 2\varepsilon_h)$, ε_h being the permittivity of host medium. Thus we can write the equation for the field enhancement factor of the pump $x_0(\omega_0)$

$$x_0(\omega_0) = \frac{3\varepsilon_h}{\varepsilon_{m0} + 2\varepsilon_h + \chi_m^{(3)} \left|x_0(\omega_0) E_0\right|^2}, \quad (4)$$

which we solve numerically [17]. By using the standard Maxwell-Garnett theory [21] and the above equations, we obtain the effective dielectric function for the probe. For larger or non-spherical NPs, we apply the discrete dipole approximation in combination with the effective medium approximation [17] by using Eqs. (3, 4). The term $1 + \frac{1}{1+i\Omega\tau}$ in Eq. (3) for $\varepsilon_m(\omega_{pr})$ leads to a narrow spectral dip in the loss coefficient and the refraction index, the width of which is given by τ^{-1}, arising from the coherent coupling of the probe with the pump.

Let us first demonstrate the above described principal mechanism of slow light for the simplest case of spherical metallic NPs permitting the application of the Maxwell-Garnett formalism. Figure 1(a) shows an example of the creation of an absorption dip and the corresponding strong dispersion of the refractive index in a layer of silica glass doped with Ag nanospheres smaller than 10 nm for a pump with an intensity of 400 MW/cm^2 at the plasmon resonance wavelength of 414.7 nm. The dielectric function of silver is taken from Ref. [22] and its nonlinear susceptibility $\chi_m^{(3)} = -(6.3 - i1.9) \times 10^{-16}$ m^{2}V^{-2} [23]. The refractive index of silica is 1.47 and the electron-phonon coupling time $\tau = 1.23$ ps [19]. The filling factor is 3×10^{-2}. The transmittance for the probe strongly increases near $\Omega = 0$ and drops for higher Ω. As the plasmonic dephasing time is in the range of few femtoseconds, the width of the dip is more than 100 times narrower than the plasmon bandwidth. This narrow transparency window in the plasmonic absorption spectrum leads to strong dispersion and a large decrease of the group velocity near $\Omega = 0$ due to the Kramers-Kronig relation. Note that in certain parameter regions the imaginary part of $\varepsilon_m(\omega_{pr})$ can be negative and correspondingly the absorption dip change over into a

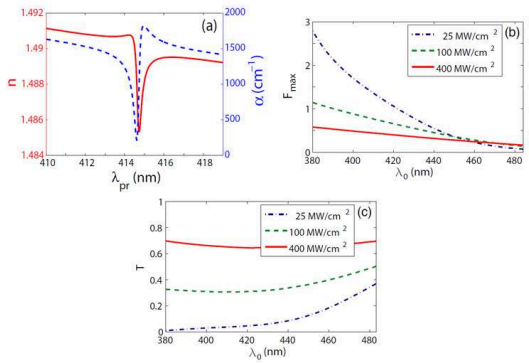

FIG. 1: (Color online) Creation of absorption dip and strong dispersion of refractive index (a) by frequency-dependent coherent energy transfer from pump to probe, maximum fractional delay (b) and transmission (c) as functions of the pump wavelength for different pump intensities in a silica glass layer doped with very small Ag nanospheres. In (b) and (c), the filling factor is 2.5×10^{-2}, the propagation length is 2 μm, $\tau = 1.23$ ps.

gain peak. For spherical particles this occurs if the condition $\mathrm{Im}\left[\varepsilon_{\rm m}(\omega_0)\right] < \left|\chi_{\rm m}^{(3)} \left(\mathrm{E}_0^{\rm enh}\right)^2\right| \Omega\tau / \left[1 + (\Omega\tau)^2\right]$ for purely real $\chi_m^{(3)}$, requiring stronger pump in practice due to the non-zero imaginary part of $\chi_m^{(3)}$. For spherical NPs with the above given parameters, this condition requires a rather high intensity in the range of 10 GW/cm^2. However, as will be shown later for gold nanorods the same effect occurs also for non-spherical particles. Since the plasmon resonance for nanorods can be shifted to the IR spectral range exhibiting the much higher value of $\left|\chi_m^{(3)}\right|$, a gain peak is already created for even much smaller intensities in the range of 0.3 MW/cm^2.

Figures 1(b) and (c) show the fractional delay $F = T_{\rm del}/T_0$ and the transmission T as functions of the pump wavelength for different pump intensities. Here $T_{\rm del}(\omega_{pr}) = L\left(v_g^{-1} - c^{-1}\right)$ is the total delay, L the propagation length, c the light velocity in vacuum, $v_g = c/n_g$ the group velocity, $n_g = d\left[n(\omega_{pr})\,\omega_{pr}\right]/d\omega_{pr}$ the group index with the effective index $n(\omega_{pr})$, and T_0 is the pulse duration. The filling factor is 2.5×10^{-2}, the propagation length is 2 μm, and the duration of the probe pulse is 1.85 ps, which is around 1.5 times longer than the electron-phonon coupling time τ. The other parameters are the same as in Fig 1(a). One can see that the fractional delay increases with increasing intensity while the transmission shows an opposite behavior. As can be seen, for pump intensities below 300 MW/cm^2 the delay decreases with increasing pump wavelength while the transmission increases.

For practical applications, it is worth to study slow-light performance at telecommunication wavelengths. The plasmon resonance can be shifted to a large extent by tailoring the shape of the metallic NPs, in particular nanorods are suitable to shift the plasmon resonance into the long

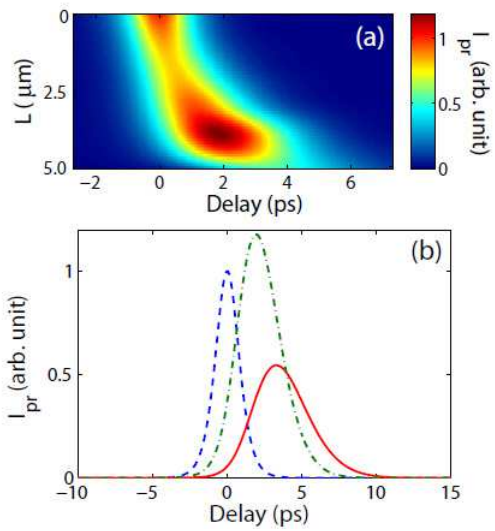

FIG. 2: (Color online) Slow light in TiO_2 film doped with Au nanorods with a diameter of 20 nm and a length of 66 nm for pump intensity of 6 MW/cm^2 at 1550 nm. Other parameters are the same as in Fig. 3. In (a) and (b), probe pulse evolution and optical delay are shown, respectively. In (b), blue dotted line is the incident probe pulse, green dash-dotted and red solid lines are probe pulses corresponding to propagation lengths of 4 and 5 μm.

wavelength range. In this wavelength range, noble metals have extremely large inherent nonlinear susceptibilities, e. g. for gold -1.5×10^{-11} m^{2}V^{-2}, which is about 4 orders larger than in the visible range [24]. To take into account the decrease of the pump intensity during the propagation due to the residual absorption and the change in the complex amplitude of probe, here we simultaneously solve the coupled propagation equations for the *cw* pump and the pulsed probe, using the effective dielectric function, calculated by the method mentioned above. The time-domain probe pulse shape then is obtained by using the Fourier transformation.

Figure 2 displays an example of the incident and delayed pulses for a pump intensity of 6 MW/cm^2 at 1550 nm. As a slow light material, we take a TiO_2 film doped with Ag nanorods with a diameter of 20 nm and a length of 66 nm, exhibiting a surface plasmon resonance at around 1540 nm. Pump and probe beams have the same propagation direction and polarization. The pulse duration was 1.85 ps , corresponding to 1.5τ. Figure 2(a) shows the evolution of probe pulse. Though the absorption for the pump is saturated, the output pump beam is attenuated down to 34 kW/cm^2 (not shown), which is $\sim$ 200 times smaller than the input pump intensity. The probe is sustained primarily by the coherent energy transfer from the pump and then it is attenuated by linear loss after the strong decrease of pump intensity. The probe energy can become even larger than the incident at a certain propagation length. The possible occurrence of a gain peak for the probe under certain conditions was discussed above; here it arise already for rather low intensities. This can be clearly seen from Fig. 2(b); the peak intensity of the probe after propagation over a length of 4 μm (green dash-dotted line) is nearly 1.2 times larger than that of the incident pulse. For a propagation length of 5 μm, the fractional delay is about 1.79, corresponding to a delay-bandwidth product of 2.68, with an energy transmittance (the energy ratio of output pulse to the incident pulse) of about 0.76. As the pulse width is broadened during the propagation in the medium, the peak intensity was decreased slightly stronger than estimated from the transmittance and was about 0.55.

The group velocity is 198 times smaller than the light velocity in vacuum. The pulse distortion was evaluated to be around 0.76 by using the formula [25, 26]

$$D = \sqrt{\frac{\int_{-\infty}^{\infty} |I_{\rm out}(t+\triangle t) - I_{\rm in}(t)|\, dt}{\int_{-\infty}^{\infty} I_{\rm out}(t+\triangle t)\, dt}}, \qquad (5)$$

where $I_{\rm in}$ and $I_{\rm out}$ are input and output probe pulse intensities normalized to have the same maximum, respectively, and $\triangle t$ is the peak delay time. Because of the large inherent nonlinear susceptibility of gold in this wavelength range, the large fractional delay is achieved even with relatively low intensities of few MW/cm^2.

Figure 3 presents the dependence of fractional delay F and transmittance T as functions of the pump intensity in the same medium as in Fig. 2 at 1550 nm. The figure shows that the fractional delay decreases with increasing pump intensity, while the transmittance increases. In particular, for higher pump intensity, the transmittance for the probe may exceed unity, indicating amplification by an energy transfer from the strong pump. This feature is a significant advantage compared with most of the known slow-light mechanism. Pulse distortion, in this case, varies from 0.8 to 0.66 with increasing intensity (not shown). Fig. 3 shows that for a given propagation length of 5 μm a fractional delay in the

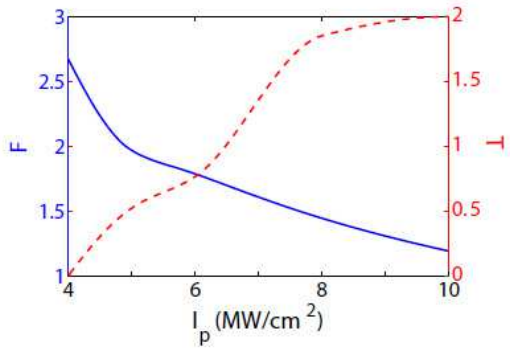

FIG. 3: (Color online) Dependencies of fractional delay F (blue solid line), transmittance T (green dotted line) on the pump intensity in TiO_2 film doped with Au nanorods at 1550 nm. The diameter and length of nanorods are 20 nm and 66 nm, respectively. The propagation length is 5 μm, the filling factor 5×10^{-2}, and the probe pulse duration 1.85 ps.

range of 2 (corresponding to a delay-bandwidth product of 3) can be obtained with a transmittance higher than 0.5.

In our knowledge, relatively few experiments in different schemes have measured relative pulses delays larger than these predictions. Comparing results obtained with chip-compatible design, we refer to Ref. [4] with a relative delay of 0.8 or to Ref. [15] with a fractional delay of 1.33. On the other hand, considerably larger fractional delays have been realized by using cascaded microring resonators using photonic wire waveguides (but with relatively small probe transmission) [14] or by using double resonances of Cs atoms [13]. However the above given numerical examples with a fractional delay in the range of 2 are not the physical limits of the method proposed in the Letter but determined by the chosen design. Next we will show that significantly larger fractional delays can be realized using a modified arrangement.

The main limitation of the delay line in collinear configuration considered up to now arises due to the limited propagation length caused by the attenuation of the pump. This can be circumvented using a transversely pumped waveguide as shown in Fig. 4(a) where the probe pulse is guided by the compact waveguide structure. The waveguide dispersion could be neglected in comparison with the dispersion arising from the NPs. The thickness of the film is taken to be 1 μm, resulting in an attenuation of the pump intensity less than 10 %, and, therefore, the pump intensity can be approximated to be constant. The other parameters are the same as in Figs. 2 and 3 except the pump intensity of 0.28 MW/cm^2. This corresponds to a pump energy of 0.2 nJ for a pump pulse duration of 200 ps, which can be considered as quasi-continuous wave in comparison with few ps duration of probe, and a transverse width of the waveguide of 5 μm. Note that the polarization directions of pump and probe have to be parallel due to the selective plasmon excitation for non-spherical NPs. Figure 4(b) presents the evolution of the probe pulse normalized to the peak intensity of the incident probe pulse. In this figure, the peak intensity of the probe increases by a factor of 3.1 after propagation over a length L of 90 μm. For detailed presentation, in Fig. 4(c) we show the normalized probe pulses corresponding to propagation lengths up to 90 μm with a equidistance of 6 μm. The figure shows a total fractional delay of about 43, corresponding to a delay-bandwidth product of 65 and a slowing down factor of around 270. The corresponding pulse distortion remains in an acceptable range with changes from 0.60 to 0.94 with increasing propagation length. In this configuration, as the probe can be amplified, we have no any principal limitation of the delay time, since with increasing propagation length and correspondingly larger pump energy the delay time can be increased significantly only limited by the available pump source.

To conclude, we proposed and studied theoretically a slow-light mechanism based on composites doped with metal NPs. If two pulses with a frequency difference

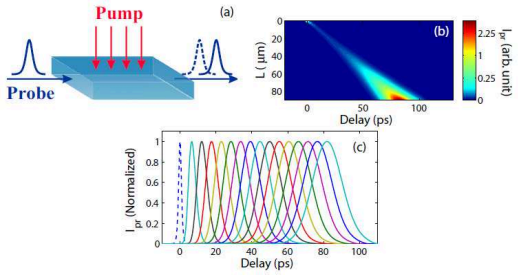

FIG. 4: (Color online) Delay for probe with a duration of 1.85 ps and pump intensity of 0.28 MW/cm^2 in TiO_2 film with thickness of 1 μm in non-collinear configuration: (a)- configuration, (b) and (c) - evolution of probe pulse. Other parameters are the same as in Fig. 3. In (c), blue dashed line is the incident pulse and solid lines are the delayed pulses corresponding to propagation lengths L up to 90 μm with a equidistance of 6 μm from the left to the right side in the order.

smaller than the electron-phonon coupling rate propagate through such a medium, plasmon-induced oscillations of the nonlinear permittivity arise, creating a strong dispersion of the effective index for the picosecond probe pulses, and correspondingly a significantly small group velocity. This scheme can be applied over a broad spectral range from visible to infrared by tailoring the sizes and shapes of the metal NPs. We have shown that employing these composites in a collinear arrangement reduced group velocities of the probe with a slow-down factor in the range of 200, a fractional delay up to more than 2.5 for probe pulses with a few ps duration can be realized as at telecommunication wavelengths using gold nanorods as well in the optical range. Avoiding pump depletion by using a non-collinear configuration, the relative delay can be significantly increased in a regime of probe amplification. We have shown that a total fractional delay of 43 (delay-bandwidth product of 65) at telecommunication wavelength can be realized in a transversely pumped waveguide geometry. Since the probe is not attenuated but can be amplified, this value of the fractional delay can be further increased with increasing length of the transversely pumped waveguide. The advantage of this configuration includes a high compactness, cost-effectiveness, broad range of applicable spectral range with tailoring the sizes and shapes of metal NPs, wide slow light bandwidth up to nearly THz, and large fractional delay. This could open the perspectives for the development of simple, compact, cheap and chip-compatible slow-light devices with large delay for applications in optical telecommunication and other fields.

* Electronic address: jherrman@mbi-berlin.de

[1] J. B. Khurgin and R. S. Tucker ed., *Slow light: science and applications* (CRC Press, Boca Raton, 2008).
[2] R.W. Boyd and D. J. Gauthier, Science **326**, 1074 (2009).

[3] L. V. Hau, S. E. Harris, Z. Dutton, and C. H. Behroozi, Nature **397**, 594 (1999).
[4] B. Wu, J. F. Hulbert, E. J. Lunt, K. Hurd, A. R. Hawkins, and H. Schmidt, Nature Photon. **4**, 776 (2010).
[5] M. S. Bigelow, N. N. Lepeshkin, and R. W. Boyd, Phys. Rev. Lett. **90**, 113903 (2003).
[6] M. S. Bigelow, N. N. Lepeshkin, and R. W. Boyd, Science **301**, 200 (2003).
[7] E. Cabrera-Granado, E. Díaz, and O. G. Caldrerón, Phys. Rev. Lett. **107**, 013901 (2011).
[8] Y. Okawachi, M. S. Bigelow, J. E. Sharping, Z. Zhu, A. Schweinsberg, D. J. Gauthier, R.W. Boyd, and A. L. Gaeta, Phys. Rev. Lett. **94**, 153902 (2005).
[9] J. Sharping, Y. Okawachi, and A. Gaeta, Opt. Express **13**, 6092 (2005).
[10] T. Baba, Nature Photon. **2**, 465 (2008).
[11] R. Hao, E. Cassan, X. L. Roux, D. Gao, V. D. Khanh, L. Vivien, D. Marris-Morini, and X. Zhang, Opt. Express **18**, 16309 (2010).
[12] J. T. Mok, C. M. De Sterke, I. C. M. Littler, and B. J. Eggleton, Nature Phys. **2**, 775 (2006).
[13] R. M. Camacho, M. V. Pack, J. C. Howell, A. Schweinsberg, and R. W. Boyd, Phys. Rev. Lett. **98**, 153601 (2007).
[14] F. Xia, L. Sekaric, and Y. Vlasov, Nature Photon. **1**, 65 (2007).
[15] Y. Okawachi, M. A. Foster, J. E. Sharping, A. L. Gaeta, Q. Xu, and M. Lipson, Opt. Express **14**, 2317 (2006).
[16] R.A. Ganeev, and A.I. Ryasnyanskii, A.L. Stepanov, and T. Usmanov, Opt. Quantum Electron. **36**, 949 (2004).
[17] Kwang-Hyon Kim, Anton Husakou, and Joachim Herrmann, Opt. Express **18**, 21918 (2010).
[18] M. Pelton, J. Aizpurua, and G. Bryant, Laser Photon. Rev. **2**, 136 (2008).
[19] J.-Y. Bigot, V. Halt, J.-C. Merle, and A. Daunois, Chem. Phys. **251**, 181 (2000).
[20] R. M. Camacho, M. V. Pack, and J. C. Howell, Phys. Rev. A **74**, 033801 (2006).
[21] J. C. Maxwell Garnett, Philos. Trans. R. Soc. London A **3**, 385 (1904).
[22] E.D. Palik ed., *Handbook of optical constants of solids* (Academic, Orlando, 1985).
[23] E. L. Falcão-Filho and C. B. de Araújo, A. Galembeck, M. M. Oliveira, and A. J. G. Zarbin, J. Opt. Soc. Am. B **22**, 2444 (2005).
[24] E. L. Falcão-Filho, R. Barbosa-Silva, R. G. Sobral-Filho, A. M. Brito-Silva, A. Galembeck, and Cid B. de Araújo, Opt. Express **18**, 21636 (2010).
[25] H. Shin, A. Schweinsberg, G. Gehring, K. Schwertz, H. J. Chang, R. W. Boyd, Q.-H. Park, and D. J. Gauthier, Opt. Lett. **32**, 906 (2007).
[26] E. S. Bautista, E. Cabrera-Granado, and R. Weigand, Opt. Lett. **36**, 639 (2011).